Thermochimica Acta, 215 (1993) 197–209
Elsevier Science Publishers B.V., Amsterdam

Non-isothermal crystallization kinetics of *n*-paraffins: comparison of even-numbered and odd-numbered normal alkanes

Ahmed Hammami and Anil K. Mehrotra

Department of Chemical and Petroleum Engineering, The University of Calgary, Calgary, Alberta T2N 1N4 (Canada)

(Received 10 June 1992)

Abstract

Recently, a model was developed for the non-isothermal crystallization of *n*-paraffins. The model was derived based on the fundamental equation of Ozawa for non-isothermal crystallization, the surface nucleation theory, and the growth rate theory for extended chain crystals. The model was successfully tested with the differential scanning calorimetry data for even-numbered *n*-paraffins of chain lengths between thirty and fifty. In this paper, the proposed model is extended to the non-isothermal crystallization kinetics of the three odd-numbered *n*-paraffins *n*-$C_{33}H_{68}$, *n*-$C_{37}H_{76}$ and *n*-$C_{41}H_{84}$. The model is found to be equally efficient and reliable in simulating the experimental data of these odd-numbered *n*-paraffins at relatively low supercooling. The crystallization exotherms and the model parameters for odd-numbered and even-numbered *n*-paraffins are compared, and explanations are provided for the observed differences between the two groups of *n*-alkanes.

INTRODUCTION

Normal paraffin hydrocarbons are by far the major components of paraffinic wax and, therefore, the most important in determining the crystallization behaviour of waxy mixtures. Four distinct structures (hexagonal, triclinic, monoclinic and orthorhombic) describe the solid phases of all *n*-paraffins with more than nine carbon atoms in the chain [1]. Differences between even-numbered and odd-numbered *n*-paraffins emerge only when there is a tilted (triclinic or monoclinic) crystalline structure involved; these dissimilarities are due primarily to packing differences in the end-group layer [1].

Our previous paper [2] afforded a basis, both theoretical and experimental, for the analysis of non-isothermal crystallization of *n*-paraffins. The

Correspondence to: A.K. Mehrotra, Department of Chemical and Petroleum Engineering, The University of Calgary, Calgary, Alberta T2N 1N4, Canada.

proposed model combines the Ozawa equation for non-isothermal crystallization with a simple formulation for the Ozawa cooling crystallization function. According to Ozawa theory [3], the degree of crystallinity at temperature T amounts to

$$\frac{X(T)}{X_\infty} = 1 - \exp\left(\frac{-K(T)}{\lambda^n}\right) \tag{1}$$

where X_∞ is the crystallinity at termination of the crystallization process, $X(T)$ is the crystallinity at temperature T, λ is the constant cooling rate, and $K(T)$ is the Ozawa cooling crystallization function. The index n is termed the Ozawa index or the Avrami exponent and can assume a value between 1 and 4 depending on whether nucleation is homogeneous or heterogeneous, and on the number of dimensions in which the crystal growth takes place.

For the specific case of n-paraffins, the temperature dependence of the Ozawa cooling crystallization function was written in the form [2]

$$K(T) = C_1(\Delta T)^{n+1} \exp\left(\frac{-C_2}{T(\Delta T)^2}\right) \tag{2}$$

where ΔT is the degree of supercooling, C_1 is a constant not strongly temperature dependent, and C_2 is a constant associated with the free energy of nucleation. Equation (2) was derived based on the assumptions that the Ozawa cooling crystallization function is related to the Avrami overall rate of isothermal crystallization, that the crystallization is homogeneous, and that the crystal growth is one dimensional.

The above model was validated for the crystallization of the four even-numbered n-paraffins n-$C_{30}H_{62}$, n-$C_{34}H_{70}$, n-$C_{44}H_{90}$, and n-$C_{50}H_{102}$ [2]. In this paper, non-isothermal crystallization of the odd-numbered n-paraffins n-$C_{33}H_{68}$, n-$C_{37}H_{76}$ and n-$C_{41}H_{84}$ and the effect of varying cooling rates on melt crystallization are studied by differential scanning calorimetry (DSC).

EXPERIMENTAL

Samples of the three odd-numbered n-paraffins were obtained from Fluka Chemie AG (New York, USA). The purities of these compounds are listed in Table 1. All three chemicals are typically white powders.

Experiments of dynamic cooling crystallization of the samples reported here were carried out with a Mettler differential scanning calorimeter Model DSC-12E. About 4–8 mg of each chemical was weighed and carefully distributed over the crucible (sample container) base to ensure good thermal contact between the specimen and the calorimeter; the

TABLE 1

Purities and equilibrium melting temperatures for the odd-numbered *n*-paraffins

Compound	Purity	Measured T_m^o (°C) [a]
n-Triatriacontane (*n*-$C_{33}H_{68}$)	>97%	73.0
n-Heptatriacontane (*n*-$C_{37}H_{76}$)	>99%	79.1
n-Hentetracontane (*n*-$C_{41}H_{84}$)	>97%	84.1

[a] These values correspond to the return to the baseline discussed in ref. 2.

crucible was then cold welded to its cover using a mechanical crucible sealer. Each sample was heated from ambient temperature to 125°C and annealed in the molten state for at least 2 min. The melted sample was then cooled at a constant rate λ (covering the range from 1°C min^{-1} to 10°C min^{-1}) and the DSC trace was recorded. The DSC sample chamber was continuously purged with dry nitrogen. A more detailed account of the experimental procedure is given in ref. 2.

Owing to the non-isothermal nature of the experiment, the recorded temperatures must be corrected to account for the thermal lag between a point in the sample and the location at which the thermocouple measures the temperature in the calorimeter furnace. Gray [4] defined this overall temperature lag as being the sum of that inside the sample and that between the sample bottom and the calorimeter furnace. Monasse and Haudin [5] computed the thermal gradient inside thin films of *n*-paraffins (*n*-$C_{21}H_{44}$ to *n*-$C_{25}H_{52}$) using a finite difference method, by accounting for the geometry, thermal conductivity, heat capacity, solid state transition and crystallization kinetics of their specimens. Their model predicted about 1°C maximum temperature difference inside 300 μm thick samples of *n*-paraffins during an 80°C min^{-1} cooling. Therefore, the temperature lag within the *n*-paraffin samples measured at the much slower cooling rates of this work was deemed negligible. Assuming that a similar value would be obtained for the *n*-paraffins studied here, only a temperature calibration as a function of cooling rates was needed. This was achieved by calibrating the DSC with an indium standard at various scanning rates [6].

RESULTS AND DISCUSSION

Some representative crystallization exotherms of *n*-$C_{41}H_{84}$ at three cooling rates are given in Fig. 1. The actual cooling curves for this specimen are too many to show and so only those measured at 1, 5, and 10°C min^{-1} are presented. As can be seen, the baseline is the continuation of straight lines observed on DSC thermograms before and after the completion of crystallization heat evolution.

The data treatment, then, involves calculating the relative crystallinity as

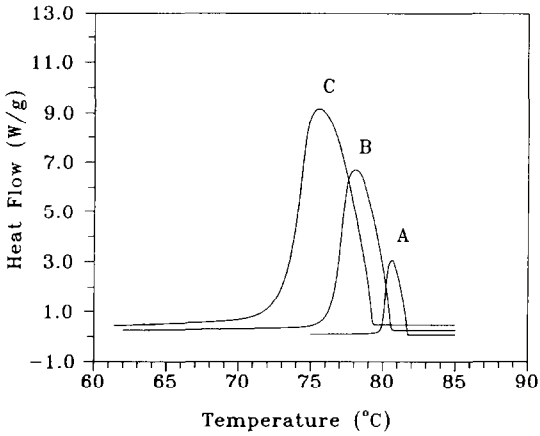

Fig. 1. Typical DSC crystallization exotherms of n-$C_{41}H_{84}$ at various cooling rates: curve A, 1°C min^{-1}; curve B, 5°C min^{-1}; curve C, 10°C min^{-1}.

a function of temperature using the relation [7]

$$\frac{X(T)}{X_\infty} = \int_{T_s}^{T} \left(\frac{dH}{dT}\right) dT \Big| \int_{T_s}^{T_e} \left(\frac{dH}{dT}\right) dT \tag{3}$$

where T_s and T_e represent the onset and end temperatures of crystallization, respectively. The numerical integrations were carried out using Simpson's rule. Figure 2 shows the calculated relative crystallinity values which correspond to the cooling exotherms of Fig. 1. As in the case of even-numbered n-paraffins [2], all the curves of relative crystallinity versus temperature have essentially the same shape, which means that only the retardation effects of cooling rate on crystallization are observed for these curves.

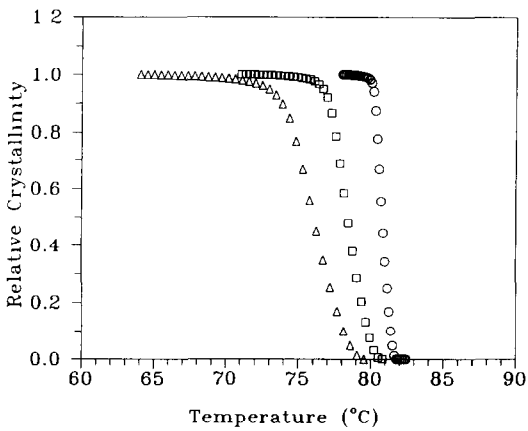

Fig. 2. Plot of relative crystallinity as a function of temperature for n-$C_{41}H_{84}$ at various cooling rates: ○, 1°C min^{-1}; □, 5°C min^{-1}; △, 10°C min^{-1}.

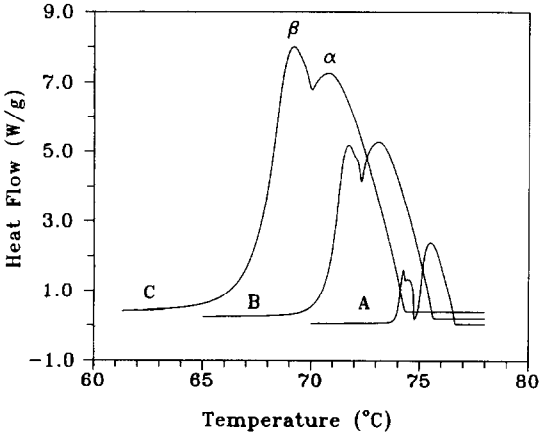

Fig. 3. Typical DSC crystallization exotherms of n-$C_{37}H_{76}$ at various cooling rates: curve A, 1°C min^{-1}; curve B, 5°C min^{-1}; curve C, 10°C min^{-1}.

Unlike n-$C_{41}H_{84}$, both n-$C_{33}H_{68}$ and n-$C_{37}H_{76}$ were observed to exhibit a solid–solid transition from the rotator crystalline phase α to the denser low temperature non-rotating solid phase β. Figures 3 (for n-$C_{37}H_{76}$) and 4 (for n-$C_{33}H_{68}$) show these transitions to be a double peak feature at all cooling rates. Broadhurst [1] has collected a set of best literature values for the temperatures and enthalpies of fusion and transition for the n-paraffins in the range 9–50 carbon atoms. He showed that odd-numbered n-paraffins with carbon number between 9 and 39 exhibit transition points in the solid state, whereas even-numbered n-paraffins show similar transitions only when their chain lengths are within the range 20–36 carbon atoms.

It is interesting to note that the solid–solid transition observed in the

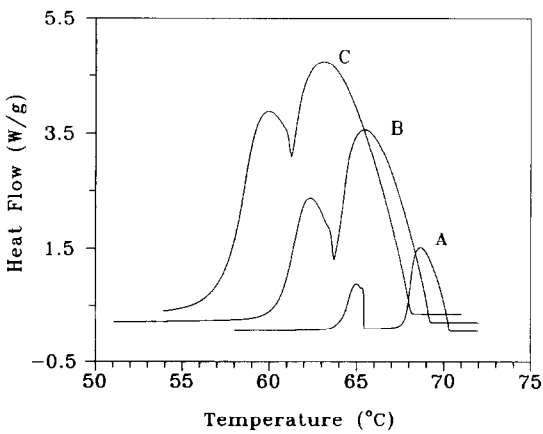

Fig. 4. Typical DSC crystallization exotherms of n-$C_{33}H_{68}$ at various cooling rates: curve A, 1°C min^{-1}; curve B, 5°C min^{-1}; curve C, 9°C min^{-1-1}.

case of n-$C_{37}H_{76}$ is somewhat different from that of n-$C_{33}H_{68}$, especially at high cooling rates. In Fig. 3, the β peak for n-$C_{37}H_{76}$ is larger than the corresponding α peak at $\lambda > 5°C\,min^{-1}$, but smaller at the slower cooling rates. In the cases of n-$C_{33}H_{68}$ (Fig. 4) and even-numbered n-paraffins n-$C_{30}H_{62}$ and n-$C_{34}H_{70}$ [2], however, the β peak remains smaller than the α peak at all cooling rates. At the present time, no satisfactory explanation can be put forward for the distinct behaviour on n-$C_{37}H_{76}$. It is possible that at low temperatures n-$C_{37}H_{76}$ crystallizes in either the monoclinic form β_M or the triclinic form β_T (i.e. tilted chain structures along the c-axis). These two tilted modifications can be of low energy for the even-numbered n-paraffins but not for the odd-numbered n-paraffins. In other words, when the paraffin chains are tilted with respect to the crystallographic ab plane, only the even-numbered n-paraffins possess the symmetry required for equivalent (apparently low energy) packing of both end groups [1]. If the above speculations are correct, n-$C_{33}H_{68}$ might crystallize in a non-tilted modification (i.e., orthorhombic β_O) for which the even and odd-numbered paraffins are equivalent and indistinguishable [1].

Another interesting characteristic of n-$C_{37}H_{76}$ (Fig. 3) is the observed sharp spikes within the β peak. Such marked shoulders are probably caused by the crystallization of a small fraction of other n-paraffins present in n-$C_{37}H_{76}$ as impurities [8]. In support of this view, Broadhurst [1] has emphasized that the usual impurities in n-paraffins are necessarily other alkanes of similar chain length because other types of impurities can be removed easily.

As discussed elsewhere [2], the solid–solid transition complicates the determination of the relative crystalinity values. It is clear from Figs. 3 and 4 that the two peaks do not separate enough for the trace to return to the baseline, except at very low cooling rates. Owing to the fact that the onset of crystallization occurs within the high temperature peak, only the α peak is important for the analyses in the present study. Following the procedure outlined in ref. 2, the completely resolved α peak (i.e. the one measured at $1°C\,min^{-1}$) was rescaled and superimposed on those which correspond to the higher cooling rate exotherms.

The calculated relative crystallinity values for the various samples were analyzed in terms of the Ozawa equation. From eqn. (1) it follows that

$$\ln\left[-\ln\left(1-\frac{X(T)}{X_\infty}\right)\right] = \ln[K(T)] + n \ln|\lambda^{-1}| \tag{4}$$

If we plot the left-hand side of eqn. (4) against $\ln|\lambda^{-1}|$ at a fixed temperature, and if the Ozawa theory is valid, we should obtain a straight line. Parameters n and $K(T)$ can be found from the slope and the intercept of such a line. It should be realized, however, that the use of eqn. (4) requires values of relative crystallinity at a given temperature for different

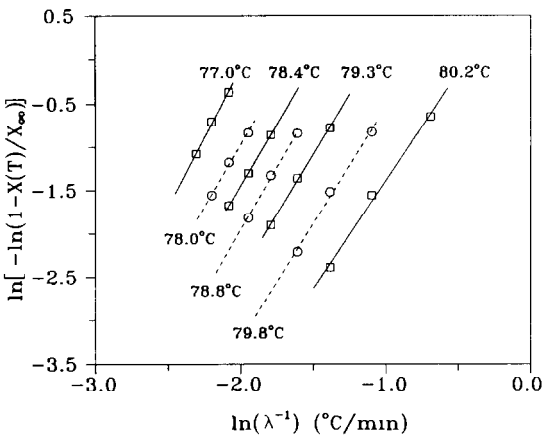

Fig. 5. Plot of $\ln[-\ln(1-X(T)/X_\infty)]$ vs. $\ln(\lambda^{-1})$ for the non-isothermal crystallization of n-$C_{41}H_{84}$ at various temperatures.

cooling rates. To cover the widest possible range of crystallization temperaures, we have applied eqn. (4) to all the experimental cooling curves, considering three consecutive cooling rates at a time.

Figures 5–7 confirm the linear trends in the data for non-isothermal crystallization of n-$C_{41}H_{84}$, n-$C_{37}H_{76}$ and n-$C_{33}H_{68}$, respectively, plotted in Ozawa coordinates according to eqn. (4). The determination of the Avrami exponent was made for the relative crystallinity values lower than 0.5. The use of higher fraction values, for which the effects of impingement and distortion of the growing crystals are quite significant, can lead to erroneous low values of n [2, 9]. Avrami exponents, determined by the least-squares method and listed in Table 2, suggest that all three pure odd-numbered

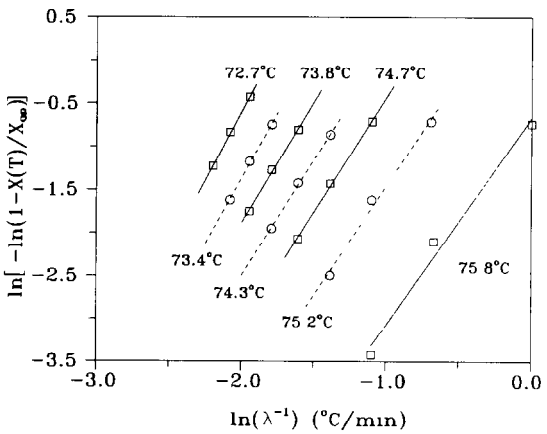

Fig. 6. Plot of $\ln[-\ln(1-X(T)/X_\infty)]$ vs. $\ln(\lambda^{-1})$ for the non-isothermal crystallization of n-$C_{37}H_{76}$ at various temperatures.

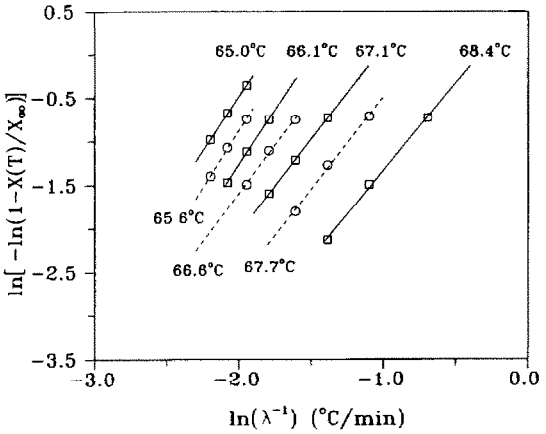

Fig. 7. Plot of $\ln[-\ln(1-X(T)/X_\infty)]$ vs. $\ln(\lambda^{-1})$ for the non-isothermal crystallization of n-$C_{33}H_{68}$ at various temperatures.

n-paraffins crystallize with homogeneous nucleation and that the crystallites grow as needles and/or plates. These morphologies are consistent with the fact that crystals grown from highly concentrated solutions or the melts of n-paraffins usually appear as bent and twisted plates, needles attached to plates, and other forms of malcrystallinity [10].

The Avrami exponents reported in Table 2 show a slight temperature dependence: they tend to decrease with increasing temperature. This behaviour, which was also observed for the even-numbered n-paraffins [2], is probably caused by localized impingements of the nuclei [9]. The non-isothermal nature of the experiment involves a progressive increase of the overall crystallization rate with decreasing temperature; as a result, molecular diffusion becomes more and more restricted giving rise to non-random distribution of the nuclei throughout the melt phase. Consequently, impingement effects are likely to occur regardless of whether the crystalline fraction is smaller than 0.5.

At a given temperature only three cooling rates were involved in generating the Ozawa plot, so it was felt more appropriate to determine the experimental values of $K(T)$ using an average Avrami exponent using the relation [2]

$$K(T_{1/2}) = \ln 2\,|\lambda|^n \tag{5}$$

where $T_{1/2}$ denotes the temperature at which 50% phase conversion is achieved. A plot of the cooling crystallization curves for the three odd-numbered paraffins is given in Fig. 8, where it is clear that $K(T)$ increases quite sharply with decreasing temperature. For comparison, the corresponding curves for the even-numbered n-alkanes [2] are also included in Fig. 8 as dashed lines.

The experimental $K(T)$ data were then analyzed in terms of eqn. (2),

TABLE 2

Avrami exponents as a function of temperature for the three odd-numbered *n*-paraffins

n-$C_{33}H_{68}$		n-$C_{37}H_{76}$		n-$C_{41}H_{84}$	
T (°C)	n	T (°C)	n	T (°C)	n
65.0	2.3	72.7	3.1	77.0	3.1
65.6	2.4	73.4	2.9	78.0	2.9
66.1	2.3	73.8	2.8	78.4	2.9
66.6	2.2	74.3	2.7	78.8	2.9
67.1	2.1	74.7	2.7	79.3	2.8
67.7	2.1	75.2	2.6	79.8	2.7
68.4	2.0	75.8	2.5	80.2	2.5

rewritten in the form [2]

$$\ln[\Psi^*(T)] = \ln C_1 - \frac{C_2}{T(\Delta T)^2} \tag{6}$$

where $\Psi^*(T)$ equals $K(T)/(\Delta T)^{n+1}$. If eqn. (2) is valid, plotting the left-hand side of eqn. (6) against $1/T(\Delta T)^2$ should yield a straight line. Parameters C_1 and C_2 can be found from the intercept and the slope of the line, respectively. Indeed, Fig. 9 affirms the linear relationship given by eqn. (6), for the three odd-numbered *n*-paraffins. The parameters $\ln C_1$ and C_2 determined by the least-squares technique are summarized in Table 3. It was shown previously [2] that C_2 values permit reasonable estimates of the lateral surface free energy ($\sigma \approx 5$ mJ m^{-2} for even-numbered *n*-paraffins). For the odd-numbered *n*-paraffins, this thermodynamic parameter was also

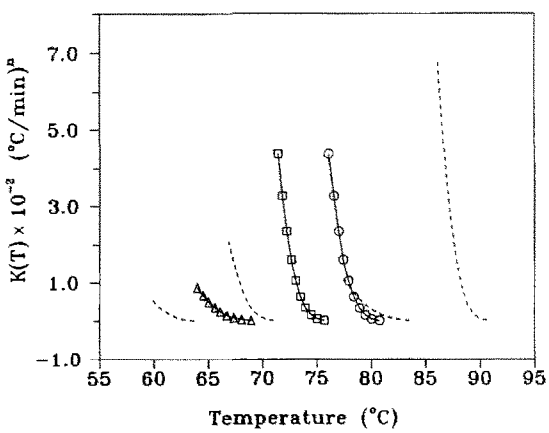

Fig. 8. Temperature dependence of the Ozawa cooling crystallization function for odd-numbered and even-numbered *n*-paraffins: ○, n-$C_{41}H_{84}$; □, n-$C_{37}H_{76}$; △, n-$C_{33}H_{68}$; - - - - (from left to right), n-$C_{30}H_{62}$, n-$C_{34}H_{70}$, n-$C_{44}H_{90}$ and n-$C_{50}H_{102}$ [2].

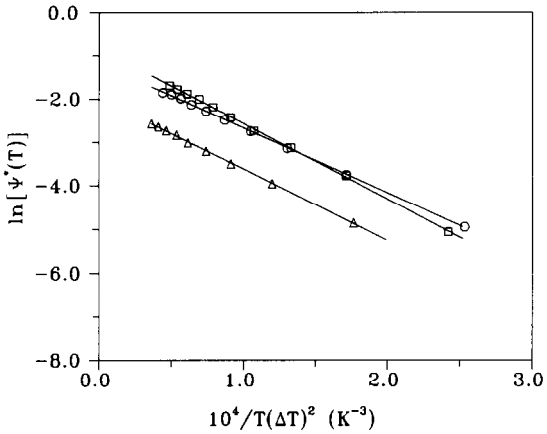

Fig. 9. Plots of $\ln[\Psi^*(T)]$ vs. $1/T(\Delta T)^2$ for the three odd-numbered n-paraffins: ○, n-$C_{41}H_{84}$; □, n-$C_{37}H_{76}$; △, n-$C_{33}H_{68}$.

TABLE 3

Parameters $\ln C_1$ and C_2 in eqn. (6) for the odd-numbered n-paraffins

Compound	n	$\ln C_1$	$C_2 \times 10^{-4}$ (K^3)	ΔH_f (J g^{-1}) [a]	σ (mJ m^{-2})
n-$C_{33}H_{68}$	2.2	−1.98	1.64	254.5	5.0
n-$C_{37}H_{76}$	2.8	−0.83	1.74	258.7	5.2
n-$C_{41}H_{84}$	2.8	−1.18	1.50	262.1	4.8

[a] Estimated, based on ref. 13.

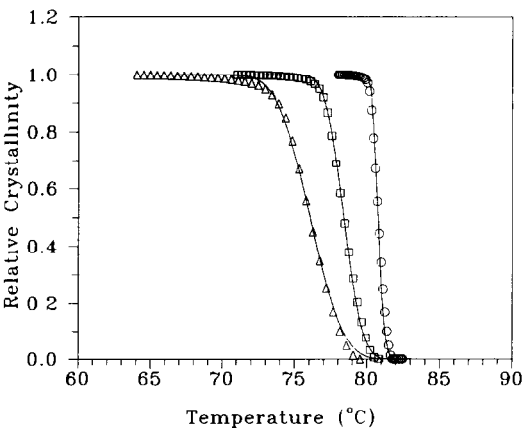

Fig. 10. Modelling the non-isothermal crystallization for n-$C_{41}H_{84}$ at various cooling rates: ○, 1°C min^{-1}; □, 5°C min^{-1}; △, 10°C min^{-1}; ——, model.

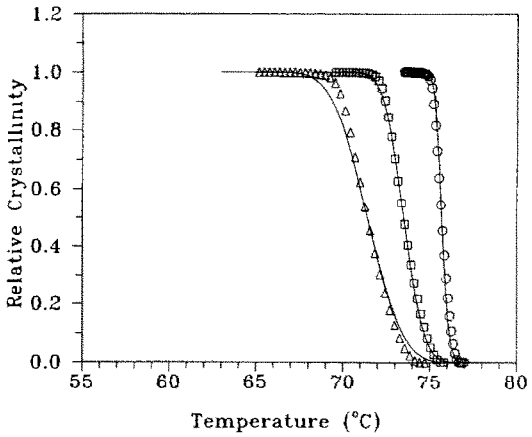

Fig. 11. Modelling the non-isothermal crystallization for n-$C_{37}H_{76}$ at various cooling rates (symbols as in caption to Fig. 10).

found to be about 5 mJ m^{-2} on average, with no systematic variation with carbon number (see Table 3). The good conformity between the results of this study and those of previous publications [2, 11, 12] is additional proof of the adequacy of eqn. (2).

Using the parameters listed in Table 3 in conjunction with eqns. (1) and (2), the experimental non-isothermal crystallization data of the three odd-numbered n-paraffins were simulated at various cooling rates, and the results are shown in Figs. 10–12. As can be seen, the model predictions follow the experimental data quite accurately, especially at low cooling rates. The slight discrepancies between the model predictions and the experimental data towards the last stages of crystallization can be attributed in large part to the fact that eqn. (2) is applicable only at relatively small

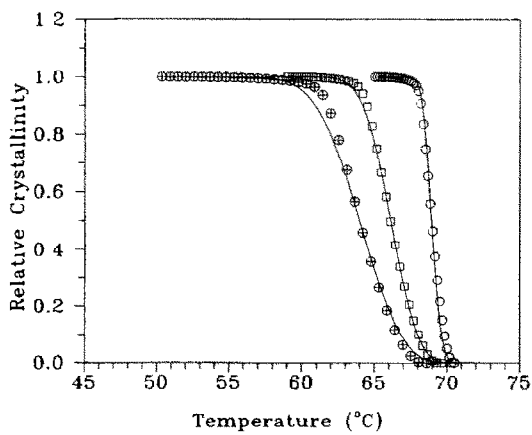

Fig. 12. Modelling the non-isothermal crystallization for n-$C_{33}H_{68}$ at various cooling rates: ○, 1°C min^{-1}; □, 5°C min^{-1}; ⊕, 9°C min^{-1}; ——, model.

degrees of supercooling ΔT (i.e. low cooling rates). Besides, it appears that such discrepancies are more pronounced for n-$C_{33}H_{68}$ and n-$C_{37}H_{76}$ than for n-$C_{41}H_{84}$. This is possibly due to the uncertainty associated with estimating the tail portion of the peaks, especially at high cooling rates, using rescaled α exotherms measured at 1°C min^{-1}.

Finally, it should be emphasized that even-numbered and odd-numbered n-paraffins do not necessarily show the same crystallization behaviour under non-isothermal conditions. Apparently, the difference is detectable by DSC only when an odd-numbered n-paraffin crystallizes in either the monoclinic or the triclinic form (i.e. tilted crystal structures) and when a solid–solid transition is involved. Nonetheless, our model can accurately describe the non-isothermal crystallization of n-paraffins, even-numbered and odd-numbered, with chain lengths between 30 and 50.

CONCLUSION

Non-isothermal crystallization of three odd-numbered n-parffins with chain lengths between 30 and 50, i.e. n-$C_{33}H_{68}$, n-$C_{37}H_{76}$ and n-$C_{41}H_{84}$ was described by the Ozawa equation. The resulting values of the Avrami exponent n, ranging from 2.0 to 3.1, suggest homogeneous nucleation and one- to two-dimensional growth of the crystallites. The proposed formulation for $K(T)$ allowed reasonable predictions of the lateral surface free energy for the three odd-numbered n-paraffins. When coupled with eqn. (2), the Ozawa equation gave remarkably good predictions of the experimental data at various cooling rates for n-paraffins with carbon numbers in the range 30–50.

ACKNOWLEDGMENTS

Financial support was provided by the Natural Sciences and Engineering Research Council of Canada (NSERC) and the Department of Chemical and Petroleum Engineering (University of Calgary).

REFERENCES

1 M.G. Broadhurst, J. Res. Natl. Bur. Stand., Sect. A, 66(3) (1962) 241.
2 A. Hammami and A.K. Mehrotra, Thermochim. Acta, 211 (1992) 137.
3 T. Ozawa, Polymer, 12 (1971) 150.
4 A.P. Gray, in R.S. Porter and J.F. Johnson (Eds.), Analytical Calorimetry, Proc. Am. Chem. Soc. Symp., Plenum, New York, 1968, p. 209.
5 B. Monasse and J.M. Haudin, Coll. Polym. Sci., 246 (1986) 117.
6 A. Hammami, MS Thesis, University of Tennessee, Knoxville, 1990.
7 C.F. Pratt and S.Y. Hobbs, Polymer, 17 (1976) 12.
8 I. Bidd and M.C. Whiting, J. Chem. Soc., Chem. Commun., (1985) 543.
9 L.C. López and G.L. Wilkes, Polymer, 30 (1989) 882.

10 W.R. Turner, Ind. Eng. Chem. Prod. Res. Dev., 10 (1971) 238.
11 M.J. Oliver and P.J. Calvert, J. Crystal Growth, 30 (1975) 343.
12 J.D. Hoffman, Macromolecules, 18 (1985) 772.
13 W. Dollhopf, H.P. Grossmann and U. Leute, Coll. Polym. Sci., 259 (1981) 267.